Immunology
The Journal of cells, molecules, systems and technologies

British Society for immunology

IMMUNOLOGY ORIGINAL ARTICLE

Massive plasmablast response elicited in the acute phase of hantavirus pulmonary syndrome

Marina García,[1] Ayelén Iglesias,[2] Verónica I. Landoni,[3] Carla Bellomo,[2] Agostina Bruno,[4] María Teresa Córdoba,[4] Luciana Balboa,[1] Gabriela C. Fernández,[3] María del Carmen Sasiain,[1] Valeria P. Martínez[2,a] and Pablo Schierloh[1,a]

[1]*Laboratorio de Inmunología de Enfermedades Respiratorias, Instituto de Medicina Experimental (IMEX)-CONICET-Academia Nacional de Medicina (ANM), Ciudad autónoma de Buenos Aires, Argentina,* [2]*Laboratorio Nacional de Referencia para Hantavirus, Servicio de Biología Molecular, Instituto Nacional de Enfermedades Infecciosas, ANLIS –'Dr. Carlos G. Malbrán', Ciudad autónoma de Buenos Aires, Argentina,* [3]*Laboratorio de Fisiología de procesos Inflamatorios, IMEX-CONICET-ANM, Ciudad autónoma de Buenos Aires, Argentina and* [4]*Laboratorio de Enfermedades Tropicales, Hospital San Vicente de Paúl, Orán, Salta, Argentina*

doi:10.1111/imm.12713
Received 26 July 2016; revised 22 December 2016; accepted 11 January 2017.
[a]These authors contributed equally to this work.
Correspondence: Dr Pablo Schierloh, Pacheco de Melo 3081, Buenos Aires 1425, Argentina. Email: lp_shier@hotmail.com
Senior author: Pablo Schierloh, PhD

Summary

Beside its key diagnostic value, the humoral immune response is thought to play a protective role in hantavirus pulmonary syndrome. However, little is known about the cell source of these antibodies during ongoing human infection. Herein we characterized B-cell subsets circulating in Andes-virus-infected patients. A notable potent plasmablast (PB) response that increased 100-fold over the baseline levels was observed around 1 week after the onset of symptoms. These PB present a $CD3^{neg}$ $CD19^{low}$ $CD20^{neg}$ $CD38^{hi}$ $CD27^{hi}$ $CD138^{+/-}$ $IgA^{+/-}$ surface phenotype together with the presence of cytoplasmic functional immunoglobulins. They are large lymphocytes (lymphoblasts) morphologically coincident with the 'immunoblast-like' cells that have been previously described during blood cytology examinations of hantavirus-infected patients. Immunoreactivity analysis of white blood cell lysates suggests that some circulating PB are virus-specific but we also observed a significant increase of reactivity against virus-unrelated antigens, which suggests a possible bystander effect by polyclonal B-cell activation. The presence of this large and transient PB response raises the question as to whether these cells might have a protective or pathological role during the ongoing hantavirus pulmonary syndrome and suggest their practical application as a diagnostic/prognostic biomarker.

Keywords: Andes virus; B cell; hantavirus pulmonary syndrome; plasmablast; polyclonal activation.

Introduction

Hantavirus are enveloped three-segmented negative-sense RNA viruses, grouped in the only genus of the *Bunyaviridae* family that is transmitted without intermediate vectors. These worldwide-distributed viruses are harboured in nature by multiple mammal species belonging to the families Talpidae, Soricidae, Chiroptera and Muridae.[1] However, pathogenic hantaviruses are only known to be associated with rodent reservoirs.[2] In America, Sigmodontinae rodents are responsible for hantavirus transmission to human, causing an acute life-threatening disease: hantavirus pulmonary syndrome (HPS). This syndrome is characterized by pulmonary oedema due to capillary leakage, without evident destruction of the lung endothelial monolayer,[3] which can be followed by cardiogenic shock. In southern South America, Andes virus (ANDV) is the major causative agent of HPS and is considered one of

Abbreviations: $ANDV^{+}$ patients, Andes virus-infected patients; ANDV, Andes virus; ARS, acute respiratory/febrile symptomatic subjects; cy-Igs, intracytoplasmic immunoglobulins; HPS, hantavirus pulmonary syndrome; HS 7 dpv, healthy subjects 7 days post vaccination; HS, healthy subject; LLA, leucocyte lysate antibodies; NP, nucleoprotein; PB, plasmablast; rNP-biot, recombinant NP biotinylated; TB, tuberculosis patients; WBC, white blood cells

the most lethal human pathogens, showing a high fatality rate, as high as 40% in Argentina and 32% in Chile.[4,5] The lack of vaccines and approved specific therapies, and the ability of this particular hantavirus to be transmitted between humans has led to their classification as a Biodefence Category A pathogen as a potential agent of biological warfare.[6]

As hantavirus infections normally induce an early humoral response in humans, laboratory confirmation of HPS is generally based on positive serological test results and, consequently, very few cases need to be confirmed by the detection of viral RNA or evidence of viral antigen in tissue.[4,7–12] The immunoprotective role of such a humoral response has been verified in animal models and correlated with good prognostics in human infections.[4,11,13] In previous studies from our group, we showed that ANDV-specific IgM antibodies can be detected as soon as the first day after the onset of symptoms.[10,11] In contrast, in other acute viral diseases such as Ebola, Influenza and those caused by *Flavivirus*, the development of a humoral immune response occurs with several days of delay.[14–16] Higher titres of anti-nucleoprotein (anti-NP) specific IgGs during the acute phase of disease were strongly associated with survival of ANDV-infected patients ($ANDV^+$ patients).[11] In the same study, we observed that serum IgG-specific responses remain at high levels for at least 200 days. Subsequent studies reinforce these notions by finding long-lasting serological memory in survivors.[17,18] However, in spite of the clinical application of specific antibodies as diagnostic and prognostic tools, the B-cell response in hantavirus-infected patients has not been previously characterized.

In the steady state, circulating human B cells are mainly composed of naive and memory cells, and their relative proportions vary along ontogeny.[19,20] Very low numbers of antibody-producing plasma cells can be found in the peripheral blood of healthy subjects. These cells are CD20-negative and express high levels of CD38, and recent studies indicate that they are mainly of mucosal origin.[21] After immunization with subunit or attenuated vaccines, newly generated plasma cells appear in the circulation.[22,23] These cells are generally termed plasmablasts (PB) because they are not fully differentiated plasma cells.[20] Most PB are generated in germinal centres and induced to circulate for a short period of time until they reach a niche in bone marrow, spleen, mucosa-associated lymphoid tissues or lymph nodes.[20–24] Similarly, during the acute phase of several human viral infections, circulating PB that secrete virus-specific antibodies have been observed.[15,16,25,26] In line with this, morphologically defined 'immunoblasts' of unknown cellular lineage and uncharacterized antigen-specificity are frequently detected in blood smears from patients with HPS.[27,28]

Therefore, in the present study we sought to determine the phenotype and frequency of blood B-cell subsets in $ANDV^+$ patients from Argentina. We demonstrate for the first time that a massive PB response takes place during a human primary infection with a member of the *Bunyaviridae* family, showing differential features with respect to PB responses evoked after vaccination or other natural infections.[15,16,25,26]

Materials and methods

Study patients and healthy donors

The procedures for sampling and analysis of HPS-suspected cases were approved by the Ethics Committee from Instituto Nacional de Genética Médica from ANLIS. For healthy donors, vaccinated volunteers and *Mycobacterium tuberculosis*-infected patients, the approval was received from the Academia Nacional de Medicina, Hemocentro Buenos Aires and the F.C. Muñiz Hospital Ethic Committees, respectively. Written informed consent was obtained from all patients and volunteers before analysis. The enrolment process included patients suspected of having HPS during the period December 2013 to April 2015. Suspected HPS cases from Buenos Aires province were submitted for diagnosis confirmation to the Hantavirus National Reference Laboratory (Laboratorio Nacional de Referencia para Hantavirus, Instituto Nacional de Enfermedades Infecciosas, ANLIS-'Dr. C. G. Malbrán'). Suspected HPS cases from Hospital San Vicente de Paul (Orán, Salta province), were submitted to Laboratorio de Enfermedades Tropicales, where samples were stabilized and stored at 4° until sent to the Laboratorio Nacional de Referencia para Hantavirus for laboratory confirmation. The clinical HPS case definition included acute febrile illness (> 38·5°) together with any sign of respiratory compromise developed within the first 72 hr after hospitalization. Standardized information was required by means of the clinical/epidemiological HPS form, elaborated by the National Ministry of Health from Argentina. Cases of HPS were laboratory confirmed according to previously described criteria.[4] The HPS cases were categorized in terms of severity grades based on the following classification: Grade I for patients with prodromal symptoms without respiratory involvement; Grade II for patients with mild to moderate respiratory compromise without haemodynamic compromise; Grade III for patients with severe respiratory insufficiency with haemodynamic compromise; Grade IV for patients with severe respiratory insufficiency with refractory-to-treatment haemodynamic compromise, with a final fatal outcome.

Patient groups were named as follows: acute confirmed HPS cases infected with Andes virus as $ANDV^+$ ($n = 17$) and convalescent HPS cases at discharge as $ANDV^+$ conv ($n = 5$). Clinically suspected patients that were discarded as HPS cases were named ARS (acute respiratory/febrile symptomatic subjects, $n = 15$). As controls, healthy

subjects (HS; $n = 24$; mean age 32 years, range 18–51 years) and healthy subjects that received the seasonal influenza vaccination (Viraflu®, Sinergium Biotech, Buenos Aires, Argentina) 1 week before blood sampling (HS 7 dpv: healthy subjects 7 days post-vaccination; $n = 16$; mean age 35 years, range 23–46 years) were recruited at the IMEX-CONICET and the Hemocentro Buenos Aires. For experiments described in Fig. 6, a group of patients with pulmonary tuberculosis (TB; $n = 10$; mean age 31 years, range 19–43 years) were enrolled and diagnosed at the Muñiz Hospital, as previously described.[29]

Sample processing

Fresh anti-coagulated blood samples from suspected HPS cases ($ANDV^+$, $ANDV^+$ conv and ARS groups) were split into aliquots for laboratory confirmation[4] and for white blood cell (WBC) analysis. Serum samples were stored at −20° and blood samples for RNA extraction were stored at −80° until their analysis. For WBC analysis from all of the study groups (including HS, HS 7 dpv and TB) the blood was stabilized with Transfix reagent (Cytomark, Buckingham, UK) no later than 6 hr post-extraction, following the manufacturer's procedures, and stored at 4° until being processed. Immediately before WBC analysis, erythrocytes were lysed with Cl_2NH_4-based lysing solution (Orthoimmune, Raritan, NJ, USA).

Serology

Serum samples from suspected cases of HPS were tested by ELISA for the presence of specific IgM (μ-capture technique) and IgG antibodies against ANDV recombinant NP (rNP). The rNP was obtained as previously described.[10]

Viral load and genotyping

RNA was extracted from 200 μl of EDTA-anticoagulated blood using Trizol (Invitrogen, Carlsbad, CA, USA) and purified with the RNaid® Kit following the manufacturer's recommendations (MP Biomedicals, Santa Ana, CA, USA). Quantitative RT-PCR of ANDV RNA was performed using a MyiQ single-colour RT-PCR detection system (BioRad, Hercules, CA, USA). The primers and the probe were selected to amplify the conserved region of the S-segment of all ANDV genotypes.[30] Primers and probe for RNAseP RNA were included as internal control and run simultaneously for each sample.[31] Genetic characterization was done by amplification of S- and/or M-segment partial fragments followed by nucleotide sequencing, as previously described.[11]

B-cell subset isolation

B lymphocytes/lymphoblasts were first enriched by immunomagnetic depletion of $CD2^+$ $CD14^+$ $CD16^+$ WBC with goat anti-mouse beads (Dynabeads®, Invitrogen).[29] Then, $CD19^+$ $CD38^{high}$ (PB) and/or $CD19^+$ $CD38^{low/neg}$ (B cells) subsets were FACS-sorted using a FACS Aria™ II cell sorter system (BD, Franklin Lakes, NJ, USA).

Microscopy

Cytospin preparations of WBC or sorted B-cell subsets were performed by centrifugation for 5 min at 300 ***g***. May–Grünwald Giemsa (Merck, Kenilworth, NJ, USA) staining was analysed at 1000× magnification with immersion oil. For fluorescence microscopy, cells were fixed and permeabilized with a cytofix/cytoperm kit (BD Biosciences, San Jose, CA, USA) and blocked with 2% BSA-PBS. Cells were then stained with FITC-conjugated anti-human Igκ/λ (Cytognos, Salamanca, Spain) and counterstained with Evan's Blue, and/or Topro (Molecular Probes, Eugene, OR, USA). Alternatively, the presence of intracellular anti-NP immunoglobulins in PB was detected by incubating cells with recombinant biotinylated NP (rNP-biot) followed by staining with Cy3-conjugated streptavidin (BioLegend, San Diego, CA, USA), FITC-conjugated phalloidin and Topro (Molecular Probes).[32] Observations were performed with an inverted confocal microscope (Olympus) at 600× magnification with immersion oil. Quantifications were performed with FIJI software.[33]

Flow cytometry

The WBC were surface-stained with allophycocyanin-, FITC-, phycoerythrin-, Peridinin chlorophyll protein-Cy5.5- and Peridinin chlorophyll protein-Vio700-conjugated antibodies purchased from BD Pharmingen (anti-IgD, CD19, CD27, CD38, CD3), BioLegend (CD27, CD20), Cytognos (anti-Igκ, Igλ, CD3, CD138) and Miltenyi Biotec (CD19; Bergisch Gladbach, Germany). The PB were defined as $CD19^+$ $CD27^{high}$ $CD38^{high}$ cells gated on an extended lymphocyte gate to include blasting (FSC^{high}) cells. For intracellular protein detection, surface-stained WBC were treated with the Transcription Factor Staining Buffer Set (e-Bioscience, San Diego, CA, USA) for Ki67 or the BD Cytofix/Cytoperm™ solution (BD Biosciences) for intracellular immunoglobulins following the manufacturers' protocols. When evaluating the presence of intracellular anti-NP antibodies in the patient's PB,[32] indirect staining was performed by first incubating permeabilized cells with rNP-biot and, after washing, cells were incubated with phycoerythrin-Cy5-streptavidin (BioLegend). Data acquisition was carried out using FACScan or FACScalibur flow cytometers both equipped with CELLQUEST software (Becton Dickinson, Franklin Lakes, NJ, USA). Flow cytometry data were analysed using the FCS EXPRESS program (DeNovo Software, Glendale, CA, USA). Absolute cell counts normalized to blood volume were calculated using the CountBright® bead system (Molecular Probes, Invitrogen).

Leucocyte lysate antibody assay

To determine the relative quantity and specificity of intracellular antibodies, leucocyte lysates (LL) were obtained from all study groups (ANDV$^+$, ANDV$^+$ conv, ARS, TB, HS and HS 7 dpv) by incubating a pellet of WBC (initially present in 0·5 ml of Transfix treated blood) with 0·1 ml of PBS, 0·5% IGEPAL® and 0·5% Triton™ X-100 (Sigma, St Louis, MO, USA) for 1 hr at 4°. Nuclei and cell debris were pelleted out with a 10-min centrifugation at 4° and 1000 ***g***. Clarified supernatants (LL) were then stored frozen at −20° until ELISA tests were performed. High-bind 96-well microplates (Nuncsort) were coated overnight at 4° with 0·1 ml of CO_3-buffer dissolved rNP (5 μg/ml), human serum albumin-conjugated glycoprotein peptides (10 μg/ml, epitopes G1, G2 and G3), purified goat anti-human IgA (10 μg/ml, Kallestad Diagnostic, Chaska, MN, USA), nuclei isolated from human peripheral blood mononuclear cells (protein content 10 μg/ml),[34] tetanus toxoid (5 μg/ml, Invesbio, Vicente López, Buenos Aires, Argentina), Viraflu® trivalent influenza vaccine (5 μg/ml, Sinergium Biotech) and *Mycobacterium tuberculosis* purified protein derivative (PPD) (10 μg/ml, ANLIS, Ciudad Autónoma de Buenos Aires, Argentina). Plates were then blocked with PBS with 1% BSA and incubated overnight with the LL. After washing, plates were incubated with either rabbit horseradish peroxidase-conjugated anti-human IgM/A/G polyvalent antibody (Sigma) or goat biotinylated anti-IgA (Kallestad), followed by incubation with horseradish peroxidase-conjugated streptavidin (e-Bioscience). Development was done with 3,3′,5,5′-Tetramethylbenzidine substrate (Sigma) and read at 450–570 nm using an Asys UVM340 microplate reader (Biochrom, Cambourne, SC, UK).

Statistical analysis

Data were compiled and/or mathematically transformed using Excel (Office package, Microsoft®, Redmond, WA, USA). Statistical analysis was performed with prism 5 (GraphPad Prism, San Diego, CA, USA). Every data set was subjected to a D'Agostino–Pearson normality test before statistical comparison. When both data series to be compared or correlated followed a normal distribution, a two-tailed Student's *t*-test or Pearson correlation test was applied, respectively. For non-parametric comparison of unpaired data sets, a Mann–Whitney *U*-test or Kruskal–Wallis *H*-test with Dunn's post hoc test was applied and for paired data sets a Wilcoxon test was used. A Spearman's test was applied for non-parametric correlation analysis. For comparison of proportions, a Fisher's exact test or chi-squared test with Yate's correction was applied. *P*-values $< 0{\cdot}05$ were considered significant. For non-linear regression analysis, pre-established curve-fitting models compiled in prism 5 software were chosen based on maximum R^2 values. Throughout the manuscript, the mean plus two standard deviations (SD) of the control group data set are the default method for threshold definition. However, if we considered that this criterion was not stringent enough for a given case (i.e. the data set was without normal distribution or had too few data points), the top value of the control group defined the cut-off limit.

Results

HPS case confirmation, epidemiological data and genetic characterization of the virus

In the present study, samples from 32 consecutive suspected cases of HPS submitted to our laboratory between December 2013 and April 2015 were analysed. Seventeen patients were laboratory confirmed as acute HPS cases (ANDV$^+$) (Table 1). The remaining 15 patients with acute febrile/respiratory symptoms that were seronegative (ARS) were included as a control group (see Supplementary material, Table S1). Additional acute or convalescent samples were obtained from some members of the former group. Genetic characterization of the virus showed that all HPS cases were infected with an ANDV genotype. AND-South genotype was identified in two patients: one of them had a history of recent travel to the Andean Patagonian region and the second was a child whose father had been previously confirmed as an HPS case in the Patagonian region (case P015). This was the only paediatric case in the study group and was also the only suspected case to be caused by inter-human transmission. In all other cases the genotype matched with those previously characterized for each region.[4,10–12,17] The clinical presentation was variable among patients with HPS, requiring hospitalization in all cases: only two cases were classified as Grade I, ten cases as Grade II and five as Grade III. There were no cases from the Grade IV category (Table 1).

Virus load was uniform in most cases, showing no significant difference between patients throughout the sampling period (Table 1 and Fig. 3a). ANDV-NP-specific antibody response was mainly early and strong, showing high titres even in the first days after the onset of symptoms. Comparison of ANDV-specific IgM titres between males and females showed significantly higher titres in samples from female patients in the acute stages of infection (see Supplementary material, Fig. S1). However, ANDV-specific IgG responses did not show statistical association with any demographic or clinical feature.

Reduction of naive B-cell levels with a concomitant increase of CD19$^+$ CD27$^+$ IgD^{neg} cells in HPS

To make a wide characterization of blood B-cell subsets circulating in ANDV$^+$ patients, we performed immunophenotyping based on CD27/IgD expression

Table 1. Demographic and laboratory features of patients with confirmed hantavirus pulmonary syndrome ($ANDV^+$)

ID No	Sex	Age	Geographic origin	Days since onset of symptoms	WBC/mm^3	Anti ANDV-NP specific		$2^{\Delta Ct}$ value	ANDV genotype	Disease severity grade
						IgM titer	IgG titer			
P001	M	20	BA-SMM	11	11 200	6400	25 600	0·570	AND-BsAs	III
P001(c)				22	10 500	6400	25 600	0·637		
P002	M	42	BA-LP	11	26 300	409 600	25 600	0·559	AND-BsAs	II
P003	M	23	BA-G	6	13 100	409 600	6400	0·763	AND-BsAs	II
P003(c)				27	11 200	409 600	25 600	0·293		
P004	F	58	BA-BJ	10	22 100	409 600	6400	0·209	AND-Lec	III
P004(c)				41	9450	102 400	25 600	0·197		
P009	F	24	BA-M	13	25 050	6 553 600	25 600	0·247	AND-Plata	II
P012	F	26	RN/CH[1]	8	85 850	1 638 400	6400	0·104	AND-South	II
P014	M	48	BA-Q	9	49 600	102 400	6400	0·046	AND-BsAs	II
P015	M	2	RN-B	7	3700	1 638 400	25 600	0·004	AND-South	III
P017	M	37	BA-Lo	4	26 350	1600	100	ND	AND-BsAs	II
P017(a2)				7	18 000	6400	400	0·250		
P017(a3)				9	16 100	25 600	400	0·578		
P020	M	32	BA-La	5	8500	102 400	6400	0·768	AND-Plata	III
P024	M	36	ST-Or	14	18 900	102 400	102 400	0·075	AND-Oran	II
P027	M	22	ST-Or	12	21 550	102 400	10 2400	0·115	AND-Oran	II
P033	M	50	BA-Lo[2]	11	28 000	25 600	6400	0·090	AND-BsAs	II
P033(c)				23	27 000	25 600	25 600	0·098		
P038	M	49	ST-Or	4	2700	102 400	1600	1·223	AND-Oran	I
P038(c)				8	9450	ND	ND	0·240		
P040	M	17	ST-Or	3	16 050	102 400	6400	0·001	ND	I
P042	M	27	BA	11	9850	25 600	6400	0·096	AND-BsAs	III
P043	M	49	ST-Or	1	13 550	6400	1	0·193	AND-Oran	II

BA, Buenos Aires province; SMM, San Miguel del Monte city; LP, La Plata city; G, Glew city; M, Merlo city; BJ, Benito Juarez city; Q, Quilmes city; Lo, Lobos city; La, Lamadrid; ST, Salta province; Or, Orán city; RN, Río Negro province; B, Bariloche city; CH, Chubut province. (c): convalescent sample at discharge from hospital, (a2): second acute sample, (a3) third acute sample. ANDV genotypes: BsAs, Buenos Aires; Lec, Lechiguanas; ND, not determined.

Patients with hantavirus pulmonary syndrome were classified in terms of disease severity as follows: Grade I, patients with prodromal symptoms without respiratory involvement; Grade II, patients with mild to moderate respiratory compromise without haemodynamic compromise; Grade III, patients with severe respiratory insufficiency with haemodynamic compromise.

[1]Patient with residence in BsAs province but with history of travel to endemic areas of RN and CH provinces.

[2]Patient with possible double exposure risk in BsAs province: Lobos and Pilar localities. WBC/mm^3: white blood cells per microlitre of blood as determined by FACS.

among $CD19^+$ $CD3^{neg}$ gated lymphocytes/lymphoblasts.[29] The percentages of naive B cells – defined by surface IgD expression and lack of CD27 – were strongly reduced in $ANDV^+$ patients when compared with HS or with ARS patients (Fig. 1a,b). Notably, when five $ANDV^+$ patients were re-tested during or after remission of symptoms ($ANDV^+$ conv), we observed a significant restoration of the % of IgD^+ $CD27^{neg}$ B cells, suggesting a normalization trend. Concomitantly with the reduction of naive B cells, we observed that the % of IgD^{neg} $CD27^+$ subset – which includes PB and memory B cells that had undergone isotype switching – were strongly augmented in $ANDV^+$ patients compared with HS or with ARS. When $ANDV^+$ patients were re-tested (i.e. $ANDV^+$ conv) we observed a significant reduction of this subset, suggesting again a trend returning to basal levels (Fig. 1a,b).

The remaining minor peripheral B-cell subsets (i.e. IgD^+ $CD27^+$, unswitched memory B cells, and IgD^{neg} $CD27^{neg}$) were altered in all three patient groups with respect to HS. Unswitched memory B cells were reduced and IgD^{neg} $CD27^{neg}$ B cells were augmented in $ANDV^+$ patients, $ANDV^+$ conv and ARS patients with respect to HS.

Massive PB response in HPS

Peripheral $CD19^+$ cells exhibiting the IgD^{neg} $CD27^+$ phenotype is a complex subset composed by switched memory B cells and circulating PB.[19,20] Therefore, we then tried to identify which was the expanded subpopulation. We did not observe significant differences in percentages (%) of switched memory B cells when comparing $ANDV^+$

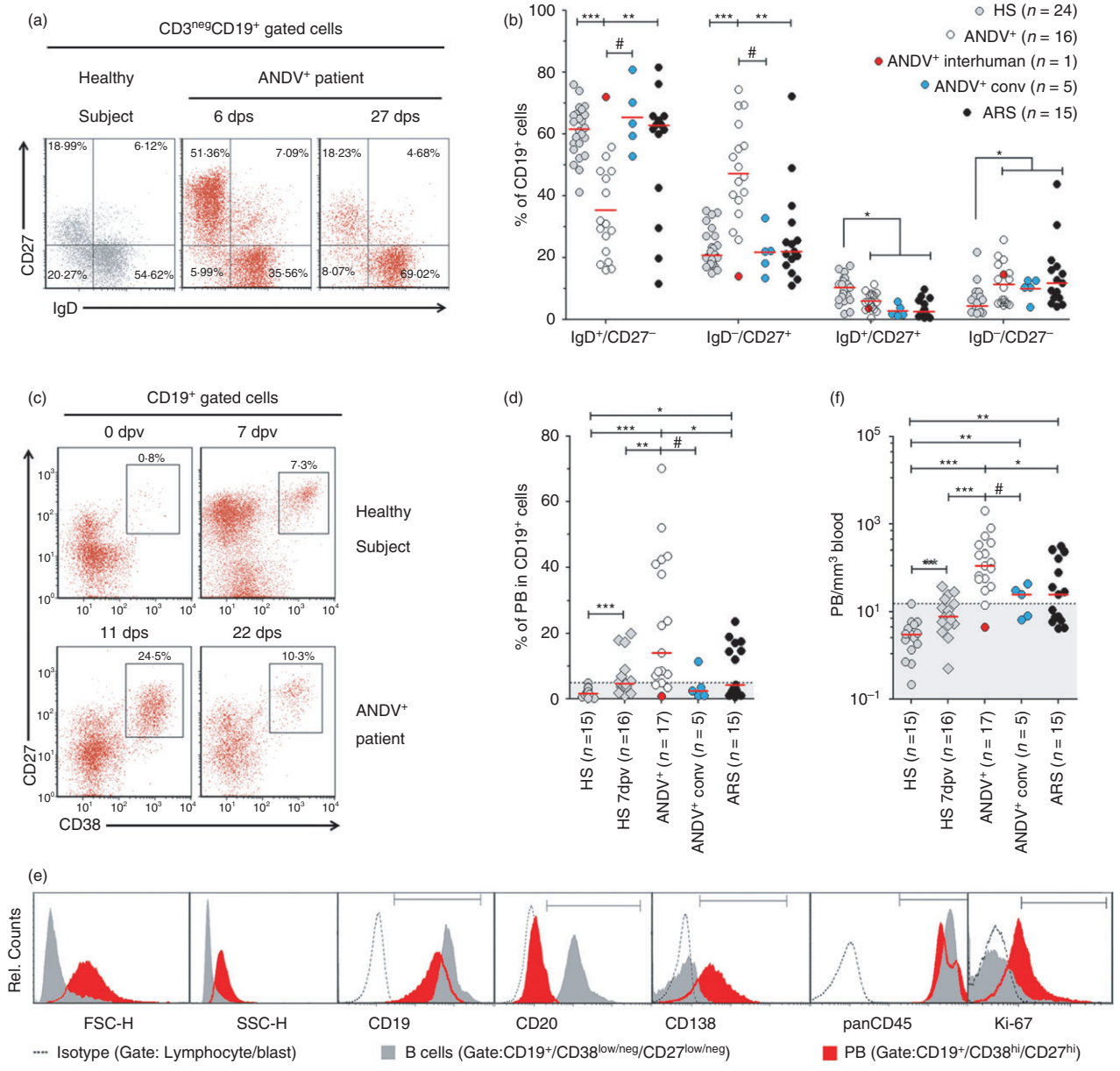

Figure 1. Elevated plasmablast (PB) levels in Andes virus (ANDV) -infected patients. (a, b) White blood cells from patients and healthy subjects (HS) were stained for CD19, CD27 and IgD and measured by flow cytometry (FACS). (a) Representative FACS analysis of a HS and an ANDV$^+$ patient [P003 and P003(c)]. Sampling dates after the onset of symptoms are indicated [6 days post onset of symptoms (6 dps) and 27 dps]. (b) Comparison of naive (IgD$^+$ CD27$^-$), switched memory or plasmablast (IgD$^-$ CD27$^+$), unswitched memory (IgD$^+$/CD27$^+$) and double-negative (IgD$^-$ CD27$^-$) B-cell populations between HS, ANDV$^+$ patients, ANDV$^+$ conv and Acute Respiratory/febrile Symptomatic (ARS) patients. (c, d) CD27 and CD38 co-staining on gated CD19$^+$ cells. Dot plots shown are gated on lymphocytes/lymphoblasts. (c) Representative analysis of the PB (CD19$^+$ CD27^{hi} CD38^{hi}) frequency in an HS and an ANDV$^+$ patient [P001 and P001(c)]. Upper graphs: analysis of CD27 and CD38 expression in a healthy subject before immunization (0 dpv) and 7 days post vaccination (7 dpv). Lower graphs: analysis of CD27 and CD38 in an ANDV$^+$ patient: 11 (11 dps) and 22 days post onset of symptoms (22 dps). (d) Comparison of percentage of PB among the CD19$^+$ cell population in HS, HS 7 dpv, ANDV$^+$, ANDV$^+$ conv and ARS. (e) Immunophenotyping of one representative ANDV$^+$ patient of five studied. FACS plots show forward scatter (FCS), side scatter (SCC) and fluorescence intensity of different cell markers (from left to right) in isotype-stained lymphocytes/lymphoblasts (dotted lines), gated B cells (grey-filled histogram) and PB (red filled histogram). (f) Comparison of absolute number of PB per microlitre of blood (PB/mm^3) in HS, HS 7 dpv, ANDV$^+$, ANDV$^+$ conv and ARS. *P < 0·05; **P < 0·005; ***P < 0·0005 (Mann–Whitney U-test). $^{\#}P$ < 0·07 (Wilcoxon). Median values are indicated by a horizontal red line. The normality range threshold (shaded grey area) was set above the HS top value. The highlighted red dot represents a 2-year-old ANDV$^+$ patient who had inter-human transmission and behaves as an outlier (P015).

patients with HS, ARS and ANDV$^+$ conv (see Supplementary material, Fig. S2a). On the other hand, the % of PB, defined as CD27^{hi} CD38^{hi} among CD19$^+$ CD3^{neg} cells, was strongly increased in ANDV$^+$ patients [median (interquartile range) = 23% (7–42%)] compared with HS and ARS (Fig. 1c,d). Interestingly, the level of PB in ANDV$^+$ conv tended to drop to normal levels, indicating a transient nature of such PB expansion. B-cell differentiation to antibody-producing cells is a stepwise process that involves changes of surface molecule expression levels together with blast-differentiation and proliferation.[20,24] Therefore, by a more detailed phenotypic analysis we confirmed that CD19$^+$ CD27^{hi} CD38^{hi} gated cells were indeed PB exhibiting increased levels of Ki67 ($P < 0{\cdot}005$, $n = 5$) and CD138 ($P < 0{\cdot}0001$; $n = 17$), lower levels of CD45 ($P < 0{\cdot}05$; $n = 5$), practically null levels of CD20 ($P < 0{\cdot}0005$; $n = 8$) and higher forward scatter ($P < 0{\cdot}0001$; $n = 17$) and side scatter ($P < 0{\cdot}0005$; $n = 17$) compared with B cells, defined as CD19$^+$ CD27$^{low/neg}$ CD38$^{low/neg}$ cells (Fig. 1e and data not shown). Additionally, a morphometric study of FACS-sorted CD19^{low} CD38^{hi} cells indicated that they were larger and had a lower nuclear to cytoplasm ratio than sorted CD19^{hi} CD38^{neg} B cells (Fig. 2).

Given that patients with HPS usually exhibit leucocytosis, mainly due to immature neutrophils,[27] we also determined the absolute number of PB per blood volume unit, confirming that it was also significantly augmented in ANDV$^+$ patients [median (interquartile range) = 135 (57–349) PB/mm^3] compared with HS [3 (1–5) PB/mm^3], ARS patients [25 (6–78) PB/mm^3] and ANDV$^+$ conv [27 (8–44) PB/mm^3] (Fig. 1f). Interestingly, the absolute number of PB/mm^3 in ANDV$^+$ conv samples remained significantly above the HS levels. Similarly, switched memory B cells/mm^3 were significantly augmented with respect to HS in all three patient groups (see Supplementary material, Fig. S2b).

Given that vaccine-evoked immune responses are accompanied by rapid PB responses that peak 1 week after immunization in adult subjects,[22,35] we decided to compare such secondary responses with the primary PB response observed in ANDV$^+$ patients. When we analysed influenza-vaccinated healthy volunteers 7 days after vaccination (HS 7 dpv; $n = 16$), we observed that % of circulating PB [median (interquartile range) = 5 (4–8) %] and absolute PB numbers [6 (4–13) PB/mm^3] were significantly lower than those in ANDV$^+$ patients (Fig. 1c, d and f). These results indicate that ANDV infection is capable of inducing a primary PB response even stronger than the memory-evoked PB response boosted by the influenza vaccine.

PB blood levels peak at the acute phase of HPS

During the acute phase of several viral human infections, reactive PB are released into the bloodstream.[15,23,26] Therefore, we correlated PB levels with patient data to look for clinically relevant associations. A peak in PB response was observed around a week after the onset of symptoms (Fig. 3a, upper graph), just before anti-NP IgG peaked and reached stable serum levels. On the other hand, no association of PB/mm^3 levels with gender, disease severity grade, geographic distribution or infecting strain and no statistically significant correlations with age, viraemia, or anti-NP IgG or IgM titres could be demonstrated herein (see Supplementary material, Fig. S3). Given that a myriad of confounders (i.e. missing data, heterogeneous population, non-systematic sampling etc.) may have introduced noise to our data, we decided to restrict the analysis to a subset of ANDV$^+$ patients that accomplished the following criteria: (i) had one sample taken during the acute phase and another taken at discharge; (ii) did not have any missing data (Table 1). In this subset of ANDV$^+$ patients we verified a strong

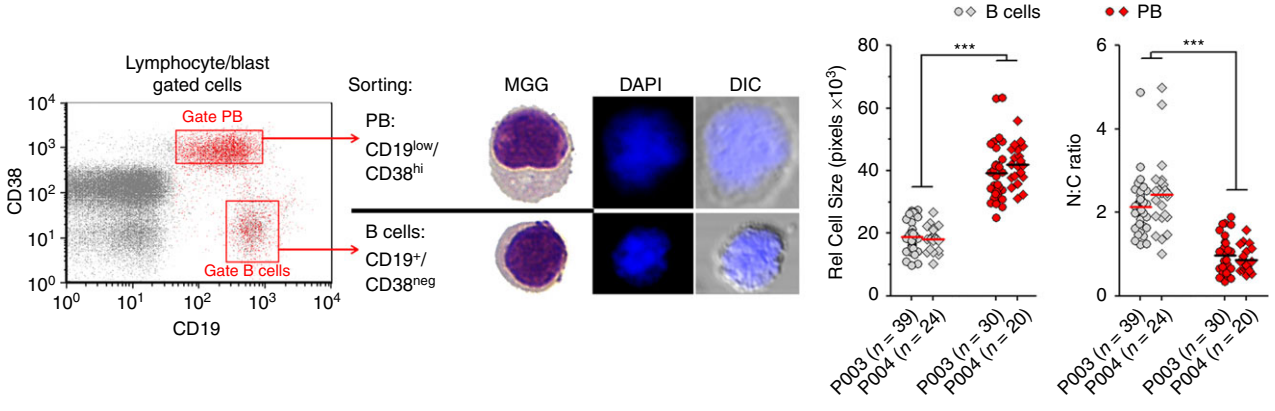

Figure 2. Morphometry of B cells and plasmablast (PB) subsets from Andes virus-positive (ANDV$^+$) patients. CD19^{low} CD38^{hi} (PB) and CD19$^+$ CD38$^{low/neg}$ (B cells) sorted cells from two representative ANDV$^+$ patient samples were stained and analysed by bright-field and fluorescence microscopy to assess differences in nuclear size and nuclear-cytoplasmic ratio. ***$P < 0{\cdot}0001$ (Mann–Whitney U-test). MGG, May–Grünwald Giemsa staining; DAPI, DNA staining with 4′,6-diamidino-2-phenylindole; DIC, Differential interference contrast.

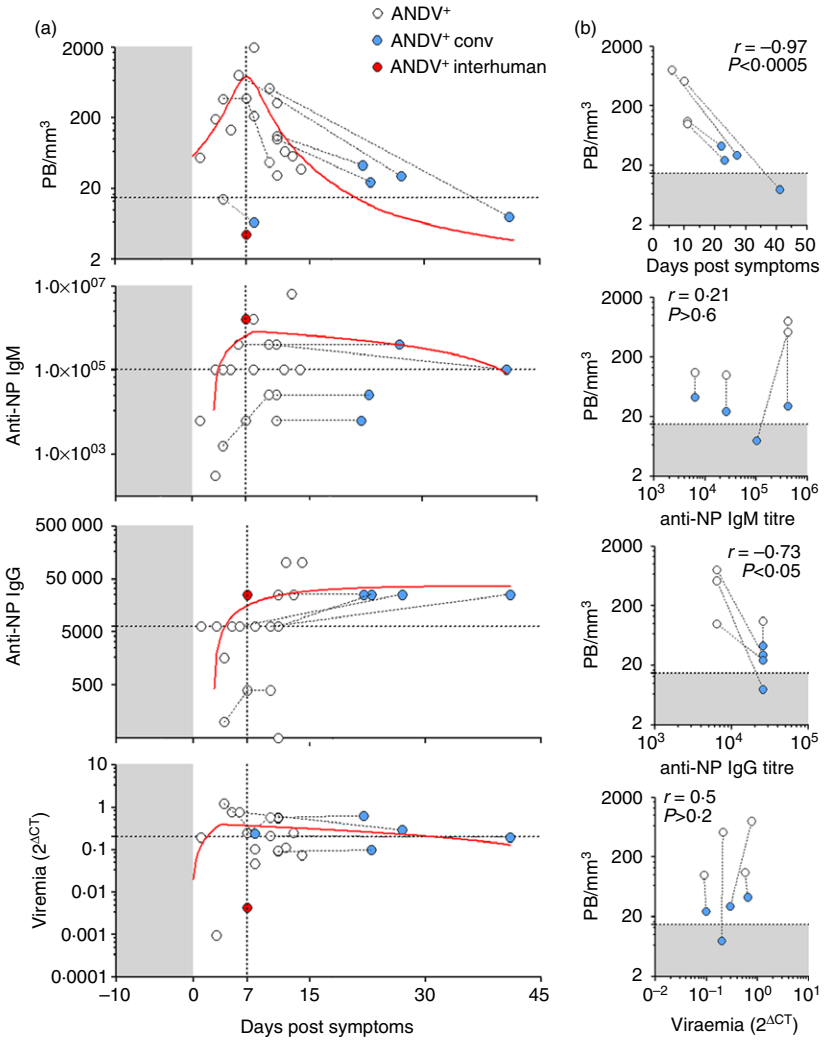

Figure 3. Andes virus-positive (ANDV$^+$) patient features in relation to blood plasmablast (PB) levels. (a) Analysis of PB levels (PB/mm^3, upper graph), IgM anti-nucleoprotein titre [IgM anti-nucleoprotein (NP) as inverse serum dilution, middle upper graph], IgG anti-NP titre (as inverse serum dilution, middle lower graph) and viraemia ($2^{\Delta CT}$, lower graph) as a function of days post onset of symptoms (dps). The red lines are the non-linear functions that best fit to the given data set. Repeated samples from a given patient are connected by dotted lines. Grey shaded areas represent incubation period. The horizontal dotted line in the upper graph was set at the normal threshold as indicated in Fig. 1(f). The horizontal dotted lines in the rest of the graphs indicate median values. The highlighted red dot represents a 2-year-old ANDV$^+$ patient who had inter-human transmission (P015). (b) Correlation analysis of PB/mm^3 with days post onset of symptoms, anti-NP IgM, anti-NP IgG and viraemia in a selected subset of ANDV$^+$ patients from whom samples were taken during acute (white dots) and convalescent (blue dots) phases of disease (i.e. P001, P003, P004 and P033). The P038 patient was excluded from this analysis given that IgM and IgG data were not available. Spearman correlation *r* factor and *P*-values are indicated. Grey shaded areas indicate normal threshold value as in Fig. 1f.

negative correlation of PB/mm^3 levels with days after the onset of symptoms ($r = -0{\cdot}97$; $P < 0{\cdot}005$) and a weaker but statistically significant negative correlation of PB/mm^3 levels with anti-NP IgG ($r = -0.\ 7$; $P < 0{\cdot}05$) (Fig. 3b). On the other hand, we did not observe any correlation with IgM or viraemia.

Increased proportion and number of IgA$^+$ PB in HPS

Given that alveolar microvascular endothelial cells are the main cellular target of New World hantaviruses,[2] we tested if PB elicited in ANDV$^+$ patients carried BALT-associated cell surface markers. As expected for a polyclonal immune reaction, we did not observe differences in κ/λ surface immunoglobulin light-chain usage when comparing peripheral B cells with PB (Fig. 4a and data not shown). In contrast, when we compared the surface IgA expression we observed that % of IgA$^+$ PB was increased with respect to % of IgA$^+$ B cells in ANDV$^+$ patients (Fig. 4a,b). Furthermore, when HS, HS 7 dpv and ARS patients were compared with ANDV$^+$ patients for IgA expression, both IgA$^+$ B cells and IgA$^+$ PB proportions (Fig. 4b) and absolute numbers (Fig. 4c) were strongly increased in the latter patient group. As observed for total PB in ANDV$^+$ patients (Fig. 3a), a blood IgA$^+$ PB peak was also observed around 1 week after the onset of symptoms (Fig. 4c). Interestingly, the levels of IgA$^+$ PB remained above normal levels in ANDV$^+$ conv samples as well. Finally, we compared the cytoplasmic IgA content of leucocyte lysates (LLA cy-IgA) from HS 7 dpv and ANDV$^+$ patients by ELISA and confirmed that the latter group had higher amounts of LLA cy-IgA (Fig. 4d).

Immunoreactivity of cytoplasmic antibodies contained in PB from patients with HPS

Because of biosafety and logistical reasons, blood samples from suspected patients with HPS needed to be fixed after collection, before analysis could be performed. This hampered the possibility of the characterization of PB

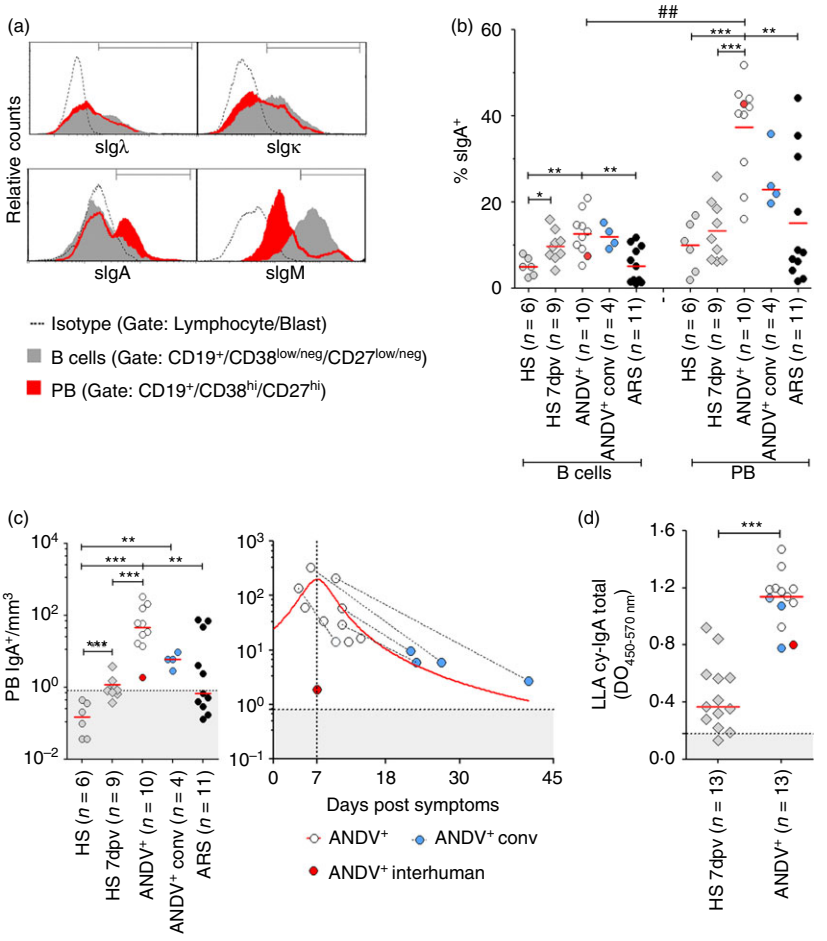

Figure 4. Frequency of IgA$^+$ plasmablasts (PB) in Andes virus-positive (ANDV$^+$) patients. (a) Immunoglobulin expression pattern of one representative ANDV$^+$ patient of ten. FACS plots of surface Igλ (sIgλ), Igκ (sIgκ), IgA (sIgA) and IgM (sIgM) in gated B cells (grey-filled histograms) and plasmablasts (PB) (red filled histograms). Isotype control gate (dotted lines) includes lymphocytes/blasts. (b) Comparison of percentage of surface IgA (% sIgA$^+$) in B cells and PB from healthy subjects (HS), HS 7 days post vaccination (dpv), ANDV$^+$ patients, ANDV$^+$ conv and Acute Respiratory/febrile Symptomatic (ARS) patients. (c) Absolute number of IgA$^+$ PB. Left: comparison of IgA$^+$ PB level in HS, HS 7 dpv, ANDV$^+$ patients, ANDV$^+$ conv and ARS patients. Right: representation of absolute IgA$^+$ PB number per microlitre of blood as a function of days after the onset of symptoms. A Lorentzian model was applied to fit the data set, achieving a coefficient of determination (R^2) = 0·42 and a peak value at day 7. (d) IgA content of white blood cell lysates (LLA cy-IgA) measured by ELISA (OD: optical density) in HS 7 dpv and ANDV$^+$ patients. The cut-off value (dotted line) corresponds to HS media + 2SD. (b, c and d) Median values are indicated by the horizontal red line and the normality threshold (HS mean + 2SD) by the grey area. The red dot represents a 2-year-old ANDV$^+$ patient who had inter-human transmission (P015). *P < 0·01; **P < 0·001; ***P < 0·0001 (Mann–Whitney U-test). $^{\#\#}P$ = 0·0005 (Wilcoxon).

effector response by standard *ex vivo* functional assays, such as ELISPOT and neutralization assays.[15,16,20–26] Therefore, instead, we analysed by confocal microscopy the intracytoplasmic immunoglobulin content of sorted PB or B cells obtained from Transfix®-treated samples. We observed that detectable amounts of intracytoplasmic immunoglobulins are present in practically all sorted PB but not in most sorted B cells from the same ANDV$^+$ sample (Fig. 5a). A similar result was obtained in samples from HS 7 dpv (see Supplementary material, Fig. S4). Next, we analysed the antigen specificity of intracytoplasmic immunoglobulins contained in sorted PB by means of rNP-biot.[32] We observed a small subset of PB-bound rNP-biot, indicating that intracytoplasmic immunoglobulins are able to recognize NP as their specific antigen (Fig. 5b). This result was further confirmed in at least four out of seven samples tested using a similar FACS-based assay which allows analysis of a larger number of PB (Fig. 5c).

Given that Transfix®-treated samples preserved the immunoreactivity of intracytoplasmic immunoglobulins in PB, as shown in Fig. 5, we designed and validated the LLA assay (see Supplementary material, Fig. S5) for testing the antigen-specificity of antibodies present in the cytoplasmic fraction of white blood cell lysates (leucocyte lysate antibodies: LLA).

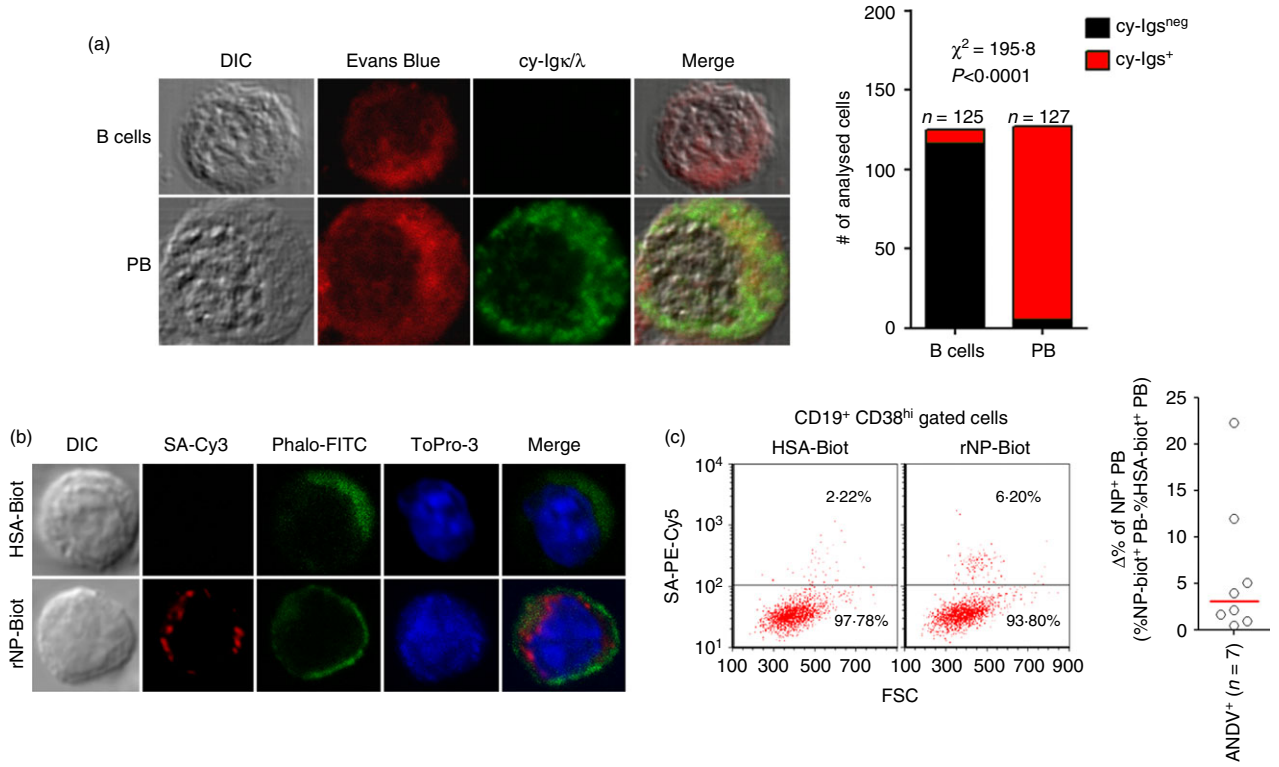

Figure 5. Immunoreactive cytoplasmic immunoglobulin (cy-Ig) in plasmablasts (PB) from Andes virus-positive (ANDV$^+$) patients. (a) Confocal microscopy analysis of sorted PB (CD19^{low} CD38^{hi}) and B cells (CD19$^+$ CD38^{neg}) was performed to assess cy-Ig content. Staining for cytoplasm [Evans Blue (EB), red] and cy-Igs (anti-Igκ/λ-FITC, green) was performed. Chi-squared analysis value is indicated. (b, c) Confocal microscopy and FACS analysis was performed to evaluate the presence of reactive cy-Igs in B lymphocytes from ANDV$^+$ patients that are able to recognize biotinylated recombinant nucleoprotein (rNP-biot). Biotinylated human serum albumin (HSA-biot) was used as a negative control. (b) Representative micrographs of purified PB (~50 cells analysed in each prepared microscope slide in two different donors) stained with phalloidin-FITC (Phalo-FITC) for cytoplasmic actin filaments (green), ToPro-3 for nuclear DNA (blue), and rNP-biot and streptavidin-Cy3 for anti-NP cy-Igs assessment. (c) Left: representative dot plots of B cells (CD19$^+$ CD38^{hi} FSC^{hi}) stained with CD19, CD38 and rNP-biot or HSA-biot and streptavidin-PE-Cy5, represented as a function of forward scatter (FSC). Right: Specific percentage (Δ%) of NP$^+$ PB was calculated by subtracting non-specific binding (i.e. HSA-biot$^+$ (SA-PE-Cy5$^+$) PB).

When using ARS samples as the negative control for setting the threshold, we observed that 69·23% of ANDV$^+$ samples tested showed detectable levels of anti-NP LLA of IgA/IgM/IgG isotypes (Fig. 6a, left graph). Furthermore, IgA anti-NP LLA were detected in 90·9% of ANDV$^+$ samples tested, perhaps because the threshold for this particular isotype was lower, enhancing the test sensitivity (Fig. 6a, right graph). Next, we analysed the presence of IgA/IgM/IgG LLA specific for three immuno-informatic predicted linear B-cell epitopes coded by glycoproteins Gn (epitopes G1 and G3) and Gc (epitope G2) (see Supplementary material, Fig. S6). We observed that 5 of the 12 tested ANDV$^+$ samples (41·67% $P = 0·0373$, Fisher's exact test) exhibited immunoreactivity against at least one epitope (Fig. 6b). Altogether these results indicate that circulating antibody-producing cells (i.e. PB and plasma cell) are able to bind virus-related antigens in most ANDV$^+$ samples.

The presence of increased levels of serum antibodies against nuclear antigens (antinuclear antibodies) and dsDNA in patients infected with European hantavirus strains indicates that B-cell responses against virus-unrelated antigens took place during Old World hantavirus infection.[36] Hence, to address possible similar bystander responses for New World hantaviruses, we performed an LLA-assay against a variety of antigens related with autoimmune responses (nuclear auto-antigens and platelet auto-antigens], vaccine responses [tetanus toxoid, Influenza neuraminidase/haemagglutinin and *Mycobacterium tuberculosis* culture-derived protein extract] and bacterial infections (lipopolysaccharides). By establishing HS samples as the negative control for setting the cut-off values, we observed that 46·67% of ANDV$^+$ samples tested showed up-normal levels of LLA against human nuclear auto-antigens (Fig. 6c, left graph). This proportion was significantly higher than the one observed for HS 7 dpv. Anti-tetanus toxoid LLA were detected in 75% of ANDV$^+$ samples, a percentage strongly superior to that observed for any other patient group (Fig. 6c, left centre graph). Unexpectedly, we observed that all ANDV$^+$

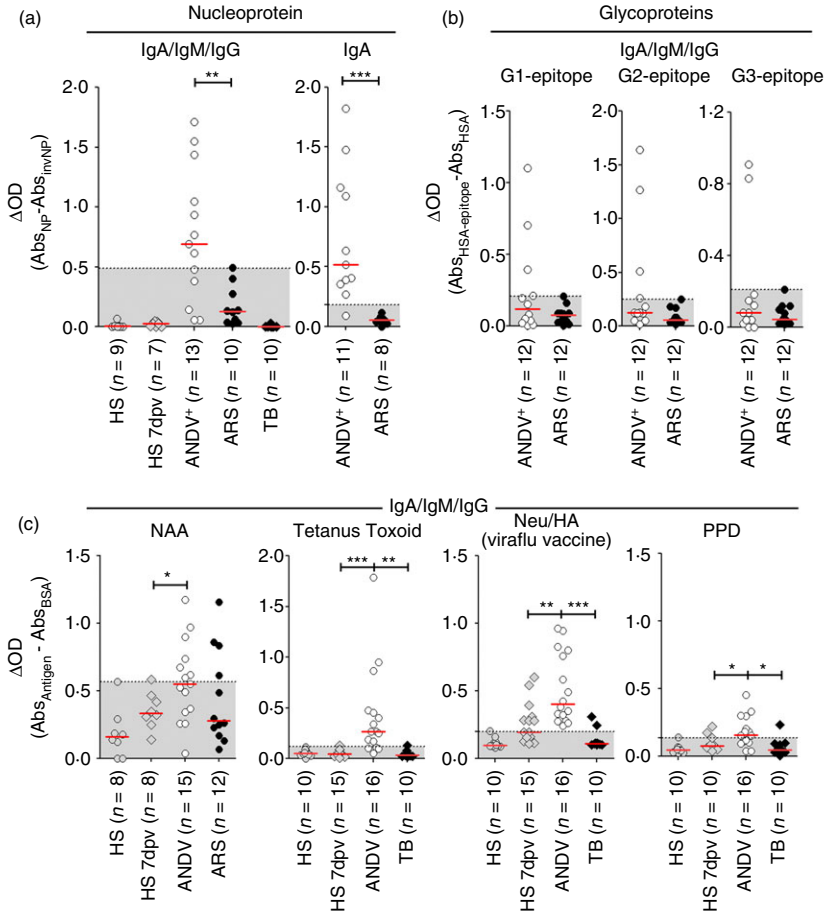

Figure 6. Plasmablasts (PB) from Andes virus-positive (ANDV$^+$) patients are reactive towards virus-specific and non-specific antigens. (a, b) Cytoplasmic fraction of white blood cell (WBC) lysates (LLA) from healthy subjects (HS), HS 7 days post vaccination (dpv), ANDV$^+$, Acute Respiratory/febrile Symptomatic subjects (ARS) and tuberculosis patients (TB) were tested by ELISA for immunoreactivity towards different ANDV antigens. (a) Anti-nucleoprotein (NP) antibodies from LLA were tested in HS, HS 7 dpv, ANDV$^+$, ARS and TB. Background signal, measured through the non-specific binding to the inverted NP (invNP) was subtracted to each data point. Positivity threshold was set above the maximum value (left graph) or mean ± 2SD (right graph) of ARS data set. (b) Presence of the anti-glycoproteins antibodies (total IgA/M/G) reactive towards computationally predicted linear B-cell epitopes (G1, G2 and G3) was tested in LLA from ANDV$^+$ and ARS patients. Background signal, measured through the non-specific binding to the carrier protein (HSA) was subtracted to each data point. (c) LLA from HS, HS 7 dpv, ANDV$^+$, ARS and TB were tested for reactivity towards virus non-specific antigens: nuclear auto-antigens (NAA), tetanus toxoid (TT), Viraflu® influenza trivalent vaccine neuraminidase and haemagglutinin (Neu/HA) proteins and *Mycobacterium tuberculosis* culture filtrate protein extract (PPD). OD, optical density. *$P < 0{\cdot}05$; **$P < 0{\cdot}005$; ***$P < 0{\cdot}0005$ (Fisher's exact test).

samples tested were positive for anti-neuraminidase/haemagglutinin LLA, showing even greater reactivity than the one exhibited by the HS 7 dpv group, which systematically received a boost immunization against those antigens 1 week before the blood sampling (Fig. 6c, right centre graph). Similarly, anti-PPD LLA were detected in a larger proportion of ANDV$^+$ samples than in patients with active pulmonary tuberculosis that are supposedly under chronic exposition to those antigens (Fig. 6c, right graph). Finally, we also observed that 50% of ANDV$^+$ samples tested showed immunoreactivity against lipopolysaccharide and that one out of nine ANDV$^+$ samples tested showed immunoreactivity against human platelets (see Supplementary material, Fig. S7). Altogether these results indicate that in ANDV$^+$ patients, circulating antibody-producing cells are able to recognize ANDV unrelated antigens.

Discussion

In an effort oriented to learn more about the immunopathogenic origin of HPS, in the present study we performed a phenotypic characterization of B-cell subsets in patients with acute HPS from endemic areas of Argentina: south, central and northwest. Remarkably, HPS is associated with a case fatality rate as high as 40% [4,5]. The cohort of patients with HPS analysed in this study includes patients with mild to severe symptoms, all of

them having been admitted to an intensive care unit. However, all patients survived, with no fatal cases included in this study. In this sense, this constituted a biased subpopulation of patients with HPS. Nonetheless, we believe that the obtained results justify this communication as a starting attempt given the difficulty in obtaining samples from patients with HPS due to the low incidence of the disease and the scattered geographical distribution of cases throughout the country.

We observed a massive PB response that peaked around 1 week after the onset of symptoms. Such magnitude and kinetics resemble what has been commonly observed during secondary immune responses (i.e. vaccine boost immunization or natural re-infections) but it is an atypical feature for most known primary infections. Interestingly, two other aggressive life-threatening viral infections (Dengue and Ebola) also produce a comparable strong PB response after primary infection.[15,26,37] One interesting case in our patient cohort was the sample from patient P015, which behaved as an outlier, closely resembling HS samples. It is important to note that this sample presented two special features that could potentially affect B-cell responsiveness. First, P015 was a paediatric patient (2 years old), suggesting that the observed PB response may be related to immune system ontogeny,[19,20] perhaps reinforcing our hypothesis that during acute ANDV infection the PB response is mediated in part by polyclonal activation of memory B cells. Second, it was a human-to-human transmission case with low viraemia together with high serum anti-NP IgG titre and a short time after the onset of symptoms (Table 1 and Fig. 3a).

The majority of the patients with HPS analysed in this study had moderate to severe symptoms, suggesting a possible role of PB in the development or resolution of the disease. Nonetheless, to further understand the meaning of PB in the pathogenesis of the disease it will be necessary to study larger patient cohorts and include patients from the Grade IV group, which have fatal outcomes.

Clinical guidelines for hantavirus infection diagnosis frequently mention the finding of 'immunoblast' cells in blood cytology examinations as a useful parameter in differential diagnosis. However, no information is provided regarding their cellular lineage.[27,28] In our study we showed using microscopy that PB that were shown to be elevated in patients with HPS coincided morphologically with those reactive blasts (Fig. 2). This, as such, constitutes a relevant finding for the hantavirus diagnostic field.

As another interesting feature, we observed high proportions of IgA^+ cells among circulating PB and B cells in patients with HPS, which is strongly suggestive of ongoing mucosal-associated humoral responses.[21,38] This particular result should be addressed in detail in future studies given the fact that New World hantaviruses exhibit a preferred lung tissue tropism.[3]

Another intriguing finding was the complex pattern of immunoreactivity observed in leucocyte lysates, which are composed of ANDV-specific and non-specific antibodies. This observation is clearly different from the mainly specific PB response seen in anti-influenza-vaccinated subjects. These results suggest that a polyclonal activation of B cells could be taking place in acute $ANDV^+$ patients as a product of a bystander effect.

A similar phenomenon has been described in patients shortly after HIV-1 infection[39] and in hospitalized acute cases of Ebola.[26] *In vitro* experiments clearly demonstrated that the signalling through pattern recognition receptors combined with certain cytokines are sufficient to induce polyclonal activation of human memory B cells and subsequent differentiation into antibody-secreting cells.[40,41] In this sense, genomic viral ssRNA, that may act as a Toll-like receptor 7/8 ligand, and B-cell-activating cytokines, such as interleukin-6, interleukin-10, vascular endothelial growth factor and B-cell-activating factor have been shown to be elevated in patients with HPS.[31,42] Another possible explanation is that B cells could constitute alternative target cells for ANDV infection, leading to their polyclonal activation, as has recently been demonstrated for Dengue virus.[43] In support of this idea, early studies show that lymphocyte subsets contain New World[3] and Old World[44] hantavirus antigens. Furthermore, recent clinical data demonstrate an increased risk for B-cell lymphoma development in people who have recovered from Puumala virus infections (ref. 45 and J. Klingström, personal communication). Nonetheless, further demonstration of PB specificity through ELISPOT assays with fresh blood samples should be performed in the future to strongly support the proposed idea of a bystander activation of B cells.

The identification of PB as reactive circulating immunoblasts (Fig. 2) together with virus antigen specificity (Figs 5 and 6) strongly suggest their practical application as a source for obtaining fully human monoclonal antibody with therapeutic potential as previously done for other viruses.[16,35,46,47] Furthermore, in endemic areas where the immunological memory against NP antigen may pose a higher false-positive rate to conventional serological tests,[48,49] PB-based diagnostic tests (i.e. ELISPOT, LLA-assay, FACS) could be useful alternative tools to differentiate ongoing infections from recovered cases. In a broader context, the LLA-assay described herein provides an easy method to monitor the B-cell effector response to Biodefense Category A viral infections (i.e. Ebola, severe acute respiratory syndrome , Lassa, ANDV and Argentine haemorrhagic fever viruses) that otherwise require Biosafety level 3 or 4 facilities for live cell-based functional assays.

As a final remark, we have described for the first time an elevated PB response in patients with HPS, which has only been reported in a few other acute viral infections, and with a magnitude that exceeds the normal PB

response observed in a secondary exposition to the same antigen (influenza-vaccinated patients). It would be of great interest for the hantavirus field to study this response in patients with hantavirus Haemorrhagic Fever with Renal Syndrome to test if a similar response is mounted in these patients and to evaluate the possible role and relevance of PB in the pathogenesis and outcome of the disease.

Author contributions

MG, VPM and PS conceived and designed the experiments. MG, AI, VL, VPM and PS performed the experiments. The collection and processing of blood samples was done by MG, AI, VL, CB, LB, AB, MTC, VPM and PS and the diagnosis of patients by AI, AB, MTC, VPM and CB. VL, CB, LB, GF, MCS, VPM and PS contributed with reagents, materials, clinical data, and/or analysis tools. The data were analysed by MG, AI, VL, VPM and PS. MG, VPM and PS wrote the paper.

Acknowledgements

We appreciate the invaluable contributions of physicians and epidemiologists in data collection and continued support, and especially of patients who gave their consent, thereby making this research possible. We are also grateful to Silvia Girard for technical support and Associate Professor Jonas Klingström and his colleagues for fruitful discussions and critical reading of the manuscript. This work was supported by grants from the National Agency for Science and Technology Promotion, Ministry of Science of Argentina (ANPCyT) – grants PICTO No 0112-2011 and PICT No 2011-0572. PS and MG are CONICET members. The funding sources had no role in the study design, data collection and analysis, decision to publish, or preparation of the manuscript.

Disclosures

The authors declare that there is no conflict of interests regarding the publication of this paper.

References

1 Guo WP, Lin XD, Wang W, Tian JH, Cong ML, Zhang HL *et al.* Phylogeny and origins of hantaviruses harbored by bats, insectivores, and rodents. *PLoS Pathog* 2013; **9**: e1003159.

2 Jonsson CB, Figueiredo LTM, Vapalahti O. A global perspective on hantavirus ecology, epidemiology, and disease. *Clin Microbiol Rev* 2010; **23**:412–41.

3 Zaki SR, Greer PW, Coffield LM, Goldsmith CS, Nolte KB, Foucar K *et al.* Hantavirus pulmonary syndrome. Pathogenesis of an emerging infectious disease. *Am J Pathol* 1995; **146**:552–79.

4 Martinez VP, Bellomo CM, Cacace ML, Suarez P, Bogni L, Padula PJ. Hantavirus pulmonary syndrome in Argentina, 1995–2008. *Emerg Infect Dis* 2010; **16**:1853–60.

5 Riquelme R, Rioseco ML, Bastidas L, Trincado D, Riquelme M, Loyola H *et al.* Hantavirus pulmonary syndrome, Southern Chile, 1995–2012. *Emerg Infect Dis* 2015; **21**:562–8.

6 He J, Kraft AJ, Fan J, Van Dyke M, Wang L, Bose ME *et al.* Simultaneous detection of CDC category "A" DNA and RNA bioterrorism agents by use of multiplex PCR and RT-PCR enzyme hybridization assays. *Viruses* 2009; **1**:441–59.

7 Jenison S, Yamada T, Morris C, Anderson B, Torrez-martinez N, Keller N *et al.* Characterization of human antibody responses to four corners hantavirus infections among patients with hantavirus pulmonary syndrome. *J Virol* 1994; **68**:3000–6.

8 Lundkvist A, Hukic M, Hörling J, Gilljam M, Nichol S, Niklasson B. Puumala and Dobrava viruses cause hemorrhagic fever with renal syndrome in Bosnia-Herzegovina: evidence of highly cross-neutralizing antibody responses in early patient sera. *J Med Virol* 1997; **53**:51–9.

9 Zoller LG, Yang S, Gott P, Bautz EK, Darai G. A novel mu-capture enzyme-linked immunosorbent assay based on recombinant proteins for sensitive and specific diagnosis of hemorrhagic fever with renal syndrome. *J Clin Microbiol* 1993; **31**:1194–9.

10 Padula PJ, Rossi CM, Della Valle MO, Martinez PV, Colavecchia SB, Edelstein A *et al.* Development and evaluation of a solid-phase enzyme immunoassay based on Andes hantavirus recombinant nucleoprotein. *J Med Microbiol* 2000; **49**:149–55.

11 Padula PJ, Colavecchia SB, Martínez VP, Gonzalez Della Valle MO, Edelstein A, Miguel SD *et al.* Genetic diversity, distribution, and serological features of hantavirus infection in five countries in South America. *J Clin Microbiol* 2000; **38**:3029–35.

12 Iglesias AA, Bellomo CM, Martínez VP. Hantavirus pulmonary syndrome in Buenos Aires, 2009–2014. *Medicina (B Aires)* 2016; **76**:1–9.

13 Bharadwaj M, Nofchissey R, Goade D, Koster F, Hjelle B. Humoral immune responses in the hantavirus cardiopulmonary syndrome. *J Infect Dis* 2000; **182**:43–8.

14 Ksiazek TG, Rollin PE, Williams AJ, Bressler DS, Martin ML, Swanepoel R *et al.* Clinical virology of Ebola hemorrhagic fever (EHF): virus, virus antigen, and IgG and IgM antibody findings among EHF patients in Kikwit, Democratic Republic of the Congo, 1995. *J Infect Dis* 1999; **179**(Suppl 1):S177–87.

15 Wrammert J, Onlamoon N, Akondy RS, Perng GC, Polsrila K, Chandele A *et al.* Rapid and massive virus-specific plasmablast responses during acute dengue virus infection in humans. *J Virol* 2012; **86**:2911–8.

16 Wrammert J, Koutsonanos D, Li G-M, Edupuganti S, Sui J, Morrissey M *et al.* Broadly cross-reactive antibodies dominate the human B cell response against 2009 pandemic H1N1 influenza virus infection. *J Exp Med* 2011; **208**:181–93.

17 Martínez VP, Colavecchia S, García Alay M, Suzuki B, Trincheri A, Busto S *et al.* Hantavirus pulmonary syndrome in Buenos Aires Province. *Medicina (B Aires)* 2001; **61**:147–56.

18 Ye C, Prescott J, Nofchissey R, Goade D, Hjelle B. Neutralizing antibodies and Sin Nombre virus RNA after recovery from hantavirus cardiopulmonary syndrome. *Emerg Infect Dis* 2004; **10**:478–82.

19 Anolik JH, Friedberg JW, Zheng B, Barnard J, Owen T, Cushing E *et al.* B cell reconstitution after rituximab treatment of lymphoma recapitulates B cell ontogeny. *Clin Immunol* 2007; **122**:139–45.

20 Caraux A, Klein B, Paiva B, Bret C, Schmitz A, Fuhler GM *et al.* Circulating human b and plasma cells. Age-associated changes in counts and detailed characterization of circulating normal CD138- and CD138 plasma cells. *Haematologica* 2010; **95**:1016–20.

21 Mei HE, Yoshida T, Sime W, Hiepe F, Thiele K, Manz RA *et al.* Blood-borne human plasma cells in steady state are derived from mucosal immune responses. *Blood* 2009; **113**:2461–9.

22 Obermoser G, Presnell S, Domico K, Xu H, Wang Y, Anguiano E *et al.* Systems scale interactive exploration reveals quantitative and qualitative differences in response to influenza and pneumococcal vaccines. *Immunity* 2013; **38**:831–44.

23 Habibi MS, Jozwik A, Makris S, Dunning J, Paras A, DeVincenzo JP *et al.* Impaired antibody-mediated protection and defective IgA B-cell memory in experimental infection of adults with respiratory syncytial virus. *Am J Respir Crit Care Med* 2015; **191**:1040–9.

24 Odendahl M, Mei H, Hoyer BF, Jacobi AM, Hansen A, Muehlinghaus G *et al.* Generation of migratory antigen-specific plasma blasts and mobilization of resident plasma cells in a secondary immune response. *Blood* 2005; **105**:1614–21.

25 Lee FE-H, Halliley JL, Walsh EE, Moscatiello AP, Kmush BL, Falsey AR *et al.* Circulating human antibody-secreting cells during vaccinations and respiratory viral infections are characterized by high specificity and lack of bystander effect. *J Immunol* 2011; **186**:5514–21.

26 McElroy AK, Akondy RS, Davis CW, Ellebedy AH, Mehta AK, Kraft CS *et al.* Human Ebola virus infection results in substantial immune activation. *Proc Natl Acad Sci USA* 2015; **112**:4719–24.

27 Koster F, Foucar K, Hjelle B, Scott A, Chong YY, Larson R *et al.* Rapid presumptive diagnosis of hantavirus cardiopulmonary syndrome by peripheral blood smear review. *Am J Clin Pathol* 2001; **116**:665–72.

28 Dvorscak L, Czuchlewski DR. Successful triage of suspected hantavirus cardiopulmonary syndrome by peripheral blood smear review: a decade of experience in an endemic region. *Am J Clin Pathol* 2014; **142**:196–201.

29 Schierloh P, Landoni V, Balboa L, Musella RM, Castagnino J, Moraña E *et al.* Human pleural B-cells regulate IFN-γ production by local T-cells and NK cells in a

Mycobacterium tuberculosis-induced delayed hypersensitivity reaction. *Clin Sci (Lond)* 2014; **127**:391–403.
30 Safronetz D, Hegde NR, Ebihara H, Denton M, Kobinger GP, St Jeor S *et al.* Adenovirus vectors expressing hantavirus proteins protect hamsters against lethal challenge with Andes virus. *J Virol* 2009; **83**:7285–95.
31 Bellomo CM, Pires-Marczeski FC, Padula PJ. Viral load of patients with hantavirus pulmonary syndrome in Argentina. *J Med Virol* 2015; **87**:1823–30.
32 Humby F, Bombardieri M, Manzo A, Kelly S, Blades MC, Kirkham B *et al.* Ectopic lymphoid structures support ongoing production of class-switched autoantibodies in rheumatoid synovium. *PLoS Med* 2009; **6**:e1.
33 Schindelin J, Arganda-Carreras I, Frise E, Kaynig V, Longair M, Pietzsch T *et al.* Fiji: an open source platform for biological image analysis. *Nat Methods* 2012; **9**:676–82.
34 Miskolci V, Hodgson L, Cox D, Vancurova I. Western analysis of intracellular interleukin-8 in human mononuclear leukocytes. *Methods Mol Biol* 2014; **1172**:285–93.
35 Li G-M, Chiu C, Wrammert J, McCausland M, Andrews SF, Zheng N-Y *et al.* Pandemic H1N1 influenza vaccine induces a recall response in humans that favors broadly cross-reactive memory B cells. *Proc Natl Acad Sci USA* 2012; **109**:9047–52.
36 Raftery MJ, Lalwani P, Krautkrämer E, Peters T, Scharffetter-kochanek K, Krüger R *et al.* Release of neutrophil extracellular traps. *J Exp Med* 2014; **211**:1485–97.
37 Sanchez A, Lukwiya M, Bausch D, Mahanty S, Sanchez AJ, Wagoner KD *et al.* Analysis of human peripheral blood samples from fatal and nonfatal cases of Ebola (Sudan) hemorrhagic fever: cellular responses, virus load, and nitric oxide levels. *J Virol* 2004; **78**:10370–7.
38 Mei HE, Frölich D, Giesecke C, Loddenkemper C, Reiter K, Schmidt S *et al.* Steady-state generation of mucosal IgA$^+$ plasmablasts is not abrogated by B-cell depletion therapy with rituximab. *Blood* 2010; **116**:5181–90.
39 Levesque MC, Moody MA, Hwang K-K, Marshall DJ, Whitesides JF, Amos JD *et al.* Polyclonal B cell differentiation and loss of gastrointestinal tract germinal centers in the earliest stages of HIV-1 infection. *PLoS Med* 2009; **6**:e1000107.
40 Bernasconi NL, Traggiai E, Lanzavecchia A. Maintenance of serological memory by polyclonal activation of human memory B cells. *Science* 2002; **298**:2199–202.
41 Pinna D, Corti D, Jarrossay D, Sallusto F, Lanzavecchia A. Clonal dissection of the human memory B-cell repertoire following infection and vaccination. *Eur J Immunol* 2009; **39**:1260–70.
42 Morzunov SP, Khaiboullina SF, St Jeor S, Rizvanov AA, Lombardi VC. Multiplex analysis of serum cytokines in humans with hantavirus pulmonary syndrome. *Front Immunol* 2015; **6**:432.
43 Correa ARV, Berbel ACER, Papa MP, Morais ATSd, Peçanha LMT, Arruda LBd. Dengue virus directly stimulates polyclonal B cell activation. *PLoS ONE* 2015; **10**: e0143391.
44 Tang YM, Yang WS, Zhang WB, Bai XF. Localization and changes of hemorrhagic fever with renal syndrome virus in lymphocyte subpopulation. *Chin Med J (Engl).* 1991; **104**:673–8.
45 Klingstrom J, Granath F, Ekbom A, Bjorkstrom NK, Ljunggren H-G. Increased risk for lymphoma following hemorrhagic fever with renal syndrome. *Clin Infect Dis* 2014; **59**:1130–2.
46 Corti D, Voss J, Gamblin SJ, Codoni G, Macagno A, Jarrossay D *et al.* A neutralizing antibody selected from plasma cells that binds to group 1 and group 2 influenza A hemagglutinins. *Science* 2011; **333**:850–6.
47 Xu M, Hadinoto V, Appanna R, Joensson K, Toh YX, Balakrishnan T *et al.* Plasmablasts generated during repeated dengue infection are virus glycoprotein-specific and bind to multiple virus serotypes. *J Immunol* 2012; **189**:5877–85.
48 Oré RMC, Forshey BM, Huaman A, Villaran MV, Long KC, Kochel TJ *et al.* Serologic evidence for human hantavirus infection in Peru. *Vector Borne Zoonotic Dis* 2012; **12**:683–9.
49 Badra SJ, Maia FGM, Figueiredo GG, Dos Santos Junior GS, Campos GM, Figueiredo LTM *et al.* A retrospective serologic survey of hantavirus infections in the county of Cássia dos Coqueiros, State of São Paulo, Brazil. *Rev Soc Bras Med Trop* 2012; **45**:468–70.

Supporting Information

Additional Supporting Information may be found in the online version of this article:

Data S1. ELISPOT assay.

Table S1. Anti-Andes virus (ANDV)-nucleoprotein antigen seronegative patients with acute respiratory and/or febrile symptoms (ARS).

Figure S1. IgM titres by gender in acute Andes virus-positive patients.

Figure S2. Switched memory B cells in Andes virus-positive patients.

Figure S3. Plasmablast response related to Andes virus-positive patients features.

Figure S4. Cytoplasmatic immunoglobulins light chains detection in circulating plasmablasts of influenza-vaccinated donors.

Figure S5. Design and validation of the leucocyte lysate antibodies (LLA) assay.

Figure S6. Bioinformatic prediction strategy and experimental validation of linear B cell-epitopes coded by Gn and Gc ectodomains from ANDV.

Figure S7. Leucocyte lysate antibodies (LLA) against human platelets and bacterial lipopolysaccharide (LPS).

Figure S8. Immunoreactivity of leucocyte lysate antibodies (LLA) against Andes virus (ANDV) antigens is not correlated with blood plasmablast (PB) levels in ANDV$^+$ patients.

